

Recovering the Reflectivity Matrix and Angle-dependent Plane-wave Reflection Coefficients from Imaging of Multiples

Alba Ordoñez PGS/UiO*, Walter Söllner PGS, Tilman Klüver PGS and Leiv J. Gelius UiO

Summary

A joint migration approach employing the complete wavefield (containing primary and multiple reflections) requires properly imaged multiples of all orders. By solving a Fredholm integral equation of the first kind, we compute the reflected impulse response (i.e., reflectivity) matrix at every image level and extract the angle-dependent plane wave reflection coefficients. We tested this imaging technique employing a simple 1D layered model with multiple reflections included. We obtained the correct Amplitude Versus Angle (AVA) response of the estimated plane wave reflection coefficient. By simultaneously imaging primaries and multiples, we also achieved an overall better image.

Introduction

In seismic acquisition primary and multiple reflections are simultaneously recorded. Historically, only primaries are used in depth migration, while multiples are treated as undesired noise. Notwithstanding, it has long been recognized that if multiples are handled in a correct way, they provide additional structural information, leading to enhanced subsurface illumination and increased image resolution (e.g., Berkhout, 1985; Mujs et al., 2007). A joint migration approach employing the complete wavefield (containing primary and multiple reflections) requires properly imaged multiples of all orders. This again demands that the reflected component of the impulse response (i.e., reflectivity) is estimated correctly at every image level.

It is well known from the literature that reflectivity can be recovered from a Fredholm integral equation of the first kind defined in the frequency-space domain (see e.g. Amundsen, 2001; Ordoñez and Söllner, 2013). From this formulation, it follows that the upgoing pressure wavefield (measured after redatuming the receivers from acquisition level to image level) can be synthesized by forming all stationary combinations of the downgoing branch of a filtered version of the vertical velocity wavefield and the reflectivity measured at the same image level, in the special case where the overburden is a homogeneous half-space. Thus, this reflectivity is the after sought quantity at each image level. Assuming that sufficient data are available, an inversion of the matrix form of this integral problem at every image level, gives an estimate of the reflectivity, where ray path interactions (i.e., crosstalk) caused by the physical overburden are eliminated. The

matrix solution of this integral problem in the frequency-space domain has already been discussed by several authors (see e.g. Berkhout, 1985; de Bruin et al., 1990). Both zero-offset and angle-dependent responses of the subsurface can be computed by choosing a convenient subset of the reflectivity matrix.

Considering separated wavefields and multiple reflections as part of the signal space, we present a controlled study to illustrate how multiples can be employed to estimate the reflectivity matrix, as well as to extract the angle-dependent plane wave reflection coefficients. Two different prestack migration experiments were carried out. First, we used source and receiver wavefields which were solely composed of multiple reflections. In the second case, we employed complete wavefields including both primary and multiple reflections.

Method

At every image level, the reflectivity can be extracted from the following Fredholm integral equation of the first kind in the frequency-space domain (Amundsen, 2001; Ordoñez and Söllner, 2013):

$$U^{(P)}(\mathbf{x}_r, \mathbf{x}_s) = -2i\omega\rho \iint_{\partial V_1} R^{IR}(\mathbf{x}_r, \mathbf{x}) D^{(V_2)}(\mathbf{x}, \mathbf{x}_s) dS, \quad (1)$$

where $U^{(P)}$ represents the upgoing pressure wavefield with the source at position \mathbf{x}_s and recorded at \mathbf{x}_r , R^{IR} is the common-receiver gather of the reflectivity (i.e. reflected impulse response) recorded at \mathbf{x}_r and with virtual sources placed along the image level at \mathbf{x} , and $D^{(V_2)}$ is the common-source gather of the downgoing vertical velocity wavefield generated at \mathbf{x}_s and recorded by virtual receivers along the same image level at \mathbf{x} . Moreover, i represents the imaginary unit, ω is the angular frequency and ρ is the mass density. In equation 1, we have used the Fourier convention: $H(\omega) = \int h(t) e^{i\omega t} dt$.

The integral problem formulated in equation 1 may be recast into a matrix representation (Berkhout, 1985; de Bruin et al., 1990). By introducing the filtered downgoing vertical velocity $D_f^{(V_2)} = -2i\omega\rho D^{(V_2)}$, we define the matrices \mathbf{R}^{IR} , $\mathbf{U}^{(P)}$ and $\mathbf{D}_f^{(V_2)}$, such as their rows correspond respectively to $R^{IR}(\mathbf{x}_r, \mathbf{x})$, $U^{(P)}(\mathbf{x}_r, \mathbf{x}_s)$ and $D_f^{(V_2)}(\mathbf{x}, \mathbf{x}_s)$ for a fixed receiver and variable source location and their columns represent the reciprocal case. Then, the integral equation 1 becomes:

Reflectivity matrix recovered from multiples

$$\mathbf{U}^{(P)} = \mathbf{R}^{IR} \mathbf{D}_f^{(V_z)} \quad (2)$$

Once the reflectivity matrix has been computed, a depth image of the subsurface can be calculated by choosing a subset of the matrix. Most one-way wave-equation migration techniques calculate only zero-offset responses. This corresponds to choosing the principal diagonal of \mathbf{R}^{IR} (Figure 1), representing the case of coinciding virtual sources and receivers in space. We then sum over frequencies to ensure the zero-time lag condition in the time-space domain. By considering other subsets of the reflected impulse response matrix, one can build common source, receiver or midpoint responses (Figure 1).

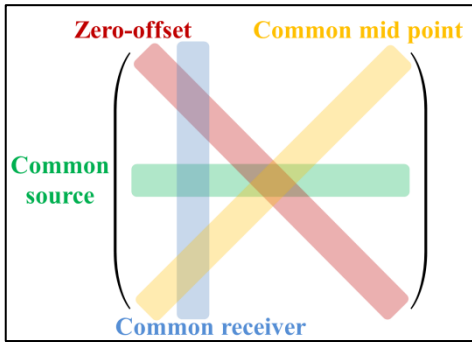


Figure 1: Structure of the reflectivity matrix.

In the following, we first determined \mathbf{R}^{IR} by least square inversion of equation 2. Then, we extracted the diagonal of the reflectivity matrix to build the zero-offset depth image (Figure 2).

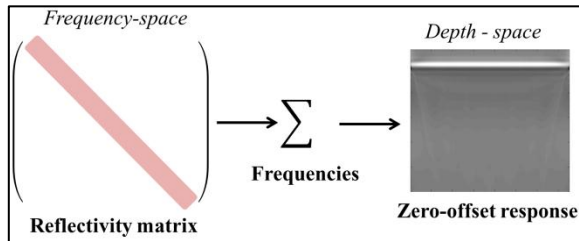


Figure 2: Workflow used to construct a zero-offset depth image.

Next, we selected the central row of the reflectivity matrix to build a common source response in the slowness domain (Figure 3). We started by Fourier transforming in the space domain so that $R^{IR}(x, \omega)$ was transformed into $\widetilde{R}^{IR}(k_x, \omega)$. Since we are after the plane-wave reflection coefficient $\widetilde{R}^{PW}(k_x, \omega)$ (defined as the ratio between the

reflected pressure and the incident pressure), $\widetilde{R}^{IR}(k_x, \omega)$ need to be scaled according to:

$$\widetilde{R}^{PW}(k_x, \omega) = 2ik_z \widetilde{R}^{IR}(k_x, \omega), \quad (3)$$

where the vertical wavenumber $k_z = \sqrt{k^2 - k_x^2}$ as usual can be expressed in terms of the horizontal wavenumber k_x and the temporal wavenumber $k = \omega/c$, c being the propagation velocity. Following de Bruin et al. (1990), we constructed an angle gather by mapping the plane-wave reflection coefficient from the wavenumber domain (k_x, ω) to the slowness domain $(p_x = k_x/\omega, \omega)$, before summing over frequencies. Note that the horizontal slowness is related to the angle ($p_x = \sin \alpha/c$).

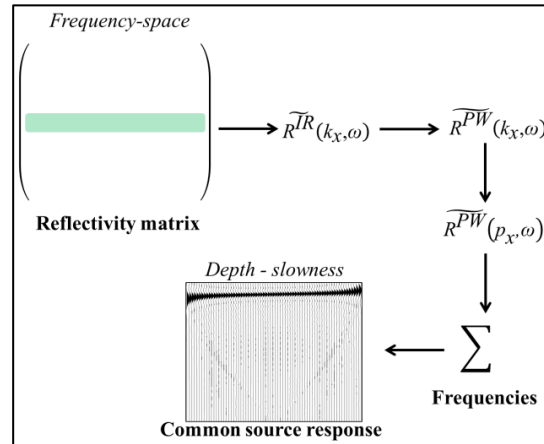


Figure 3: Workflow used to construct an angle gather.

Example

In our tests, we considered the simple 2D model presented in Table 1. The medium was composed of three layers with the two horizontal reflectors located at a depth of respectively 80 m and 200 m.

| Layer thickness (m) | Velocity (m/s) | Density (g/cm ³) |
|---------------------|----------------|------------------------------|
| 80 | 1500 | 1 |
| 120 | 1600 | 2 |
| - | 1700 | 2.4 |

Table 1: Layered model used to generate data.

For both of the two prestack migration experiments considered, we assumed a streamer depth of 25 m and generated controlled data employing a reflectivity modelling code. Each source-gather contained 150 traces separated by 12.5 m. The recording time was set to 1.5 s and the sample rate was 4 ms. The seismic source was

Reflectivity matrix recovered from multiples

located at a depth of 10 m and the source wavelet was a minimum phase Ricker wavelet with a central frequency of 15 Hz. A total of 150 shots were considered for the migrations.

Prestack migration of multiple reflections

Figure 4 displays different shot records (corresponding to the acquisition depth of 25 m) used to build up (for each frequency) the receiver wavefield matrix $U^{(P)}$. Note that only multiple reflections are considered in this case.

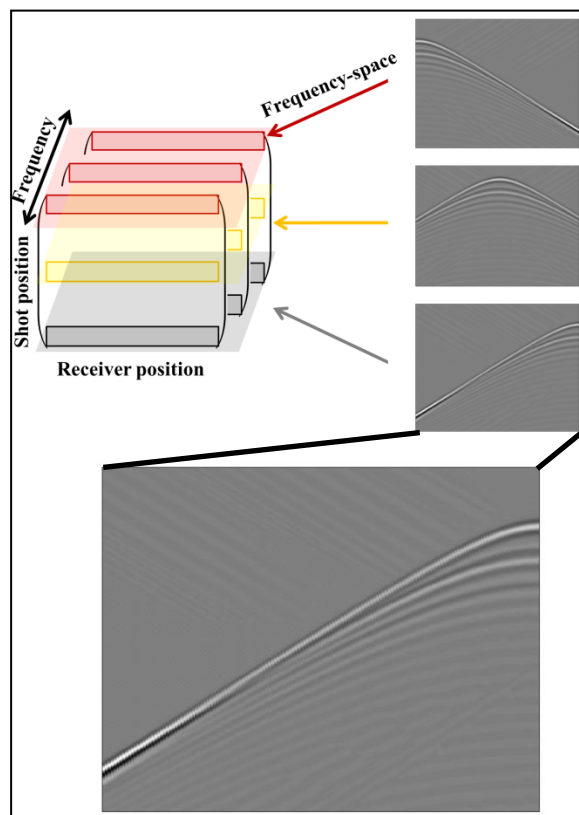


Figure 4: Structure of the receiver wavefield matrix used for the migration of multiples.

Figures 5 and 6 respectively display the zero-offset image and the angle gather obtained after migration of multiples, using the workflows of Figures 2 and 3. Figure 7 shows the amplitude picks extracted along the two events in the angle gather of Figure 6 corresponding to the two reflector depths of 80 m and 200 m. We have also superimposed the theoretical Amplitude Versus Angle response derived from the Zoeppritz equations (Aki and Richards, 1980). For the first event (Figure 7a), note that the derived response from

migration of multiples matches the theoretical response up to 56 degrees ($\sin \alpha = 0.83$). For the second event (Figure 7b), the match is acceptable up to 37 degrees ($\sin \alpha = 0.6$). The deviations observed at higher angles are due to the limited aperture.

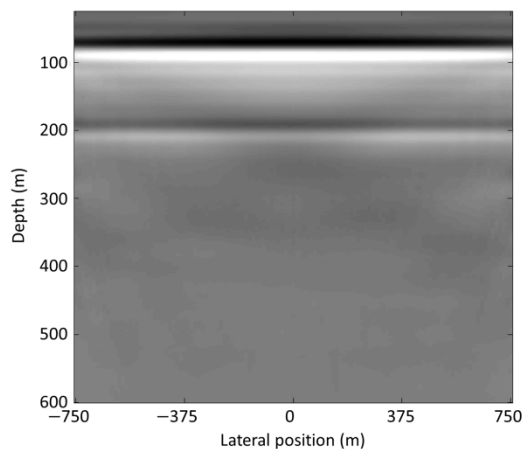


Figure 5: Zero-offset image based on multiples.

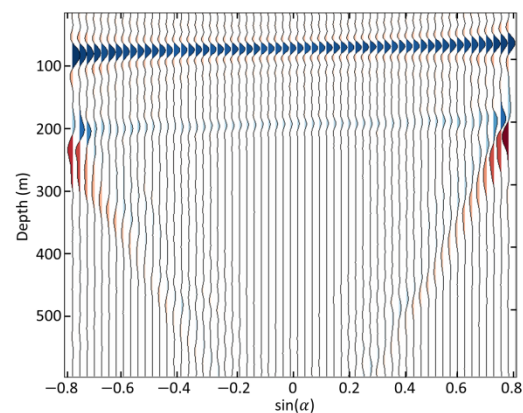
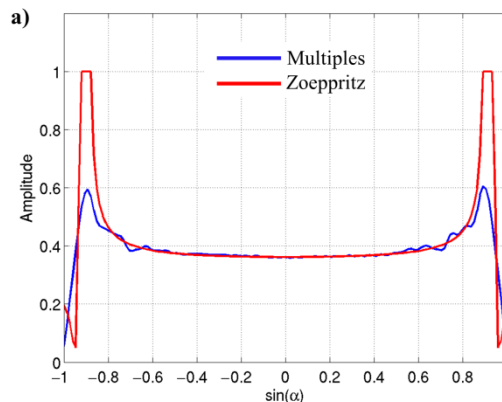


Figure 6: Angle gather formed from multiples.



Reflectivity matrix recovered from multiples

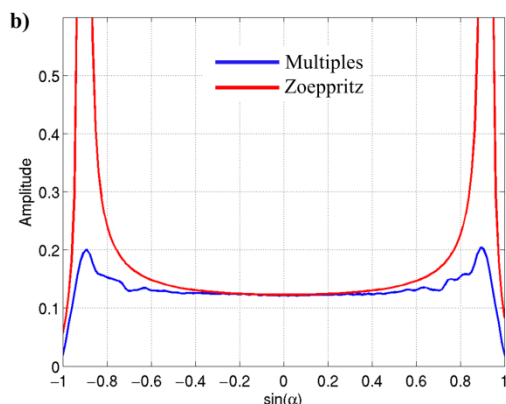


Figure 7: Amplitude picks extracted along the events at 80 m (a) and 200 m (b).

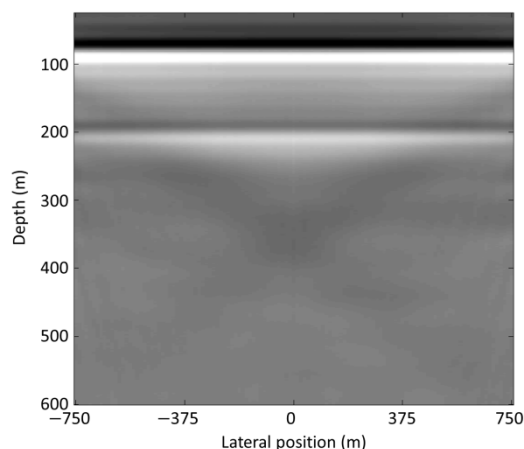


Figure 9: Zero-offset image from primaries and multiples.

Prestack migration of primary and multiple reflections

Figure 8 displays one shot record at the original acquisition depth of 25 m used to build up the monochromatic receiver wavefield matrices $U^{(P)}$. Note that both primaries and multiples are considered in this case.

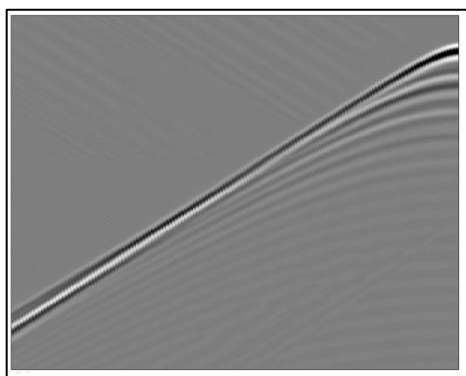


Figure 8: One shot record used for the migration of primaries and multiples.

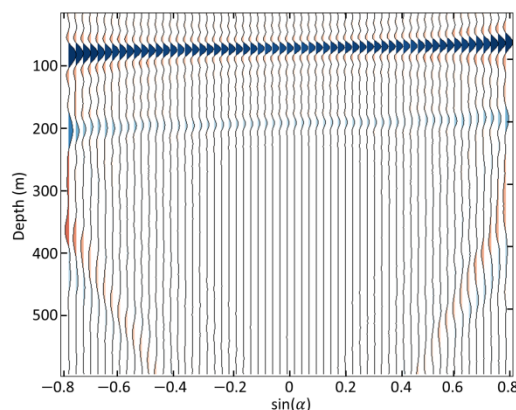


Figure 10: Angle gather from primaries and multiples.

Figures 9 and 10 respectively show the zero-offset image and the angle gather obtained after simultaneous migration of primaries and multiples. Note that there is a very good match between the depth images of the migrated multiples (Figures 5 and 6) and the simultaneously migrated primaries and multiples (Figures 9 and 10).

Conclusions

Before migration of primaries and multiples can be carried out in one step, we need to develop an imaging technique that ensures properly migrated amplitudes for all angles. In case of a simple synthetic model and considering multiples only, we computed the reflectivity matrix. By extracting particular subsets of this matrix, we demonstrated the feasibility of forming both zero-offset images and angle gathers. Indeed, the migration of multiple reflections led to a correct AVA response. We then imaged primaries and multiples simultaneously and computed the same type of responses. The use of the complete data set gave rise to an overall better image.

Acknowledgements

We thank PGS and the Department of Geosciences of UiO for permission to present this work.

<http://dx.doi.org/10.1190/segam2014-1049.1>

EDITED REFERENCES

Note: This reference list is a copy-edited version of the reference list submitted by the author. Reference lists for the 2014 SEG Technical Program Expanded Abstracts have been copy edited so that references provided with the online metadata for each paper will achieve a high degree of linking to cited sources that appear on the Web.

REFERENCES

- Aki, K., and P. G. Richards, 1980, *Quantitative seismology*: W. H. Freeman and Co.
- Amundsen, L., 2001, Elimination of free-surface related multiples without need of the source wavelet: *Geophysics*, **66**, 327–341, <http://dx.doi.org/10.1190/1.1444912>.
- Berkhout, A. J., 1985, *Seismic migration: Imaging of acoustic energy by wave field extrapolation*: Elsevier Science Publishing Company, Inc.
- de Bruin, C. G. M., C. P. A. Wapenaar, and A. J. Berkhout, 1990, Angle-dependent reflectivity by means of prestack-migration: *Geophysics*, **55**, 1223–1234, <http://dx.doi.org/10.1190/1.1442938>.
- Muijs, R., J. O. A. Robertsson, and K. Holliger, 2007, Prestack depth migration of primary and surface-related multiple reflections: Part I — Imaging: *Geophysics*, **72**, no. 2, S59–S69, <http://dx.doi.org/10.1190/1.2422796>.
- Ordoñez, A., and W. Söllner, 2013, Imaging condition for pressure-normalized separated wavefields: 75th Annual International Conference and Exhibition, EAGE, Extended Abstracts, We 02 04.